# Characterization of the novel spontaneously immortalized rat Müller cell line SIRMu-1

Thaksaon Kittipassorn, MD [a, 1]; Cameron D. Haydinger, BSc(Hons) [a]; John P.M. Wood, DPhil [b]; Teresa Mammone, MPhil [b]; Robert J. Casson, DPhil [b]; Daniel J. Peet, PhD [a,*]

[a] School of Biological Sciences, Molecular Life Sciences Building, University of Adelaide, Adelaide, SA 5005, Australia.
[b] Department of Ophthalmology and Visual sciences, Adelaide Health and Medical Sciences Building, University of Adelaide, Adelaide, SA 5000, Australia.

* Corresponding author. Assoc. Prof. Daniel J. Peet.
School of Biological Sciences, Molecular Life Sciences Building,
University of Adelaide, Adelaide, SA 5005, Australia.
Ph: +61 8 8313 5367 Fax: +61 8 8313 4362
Email: daniel.peet@adelaide.edu.au

[1] Other affiliation/permanent address. Department of Physiology, Faculty of Medicine Siriraj Hospital, Mahidol University, 2 Wanglang Road, Bangkoknoi, Bangkok, Thailand, 10700. thaksaon.kit@mahidol.ac.th.

Declarations of interest for all authors: none.

Thaksaon Kittipassorn: thaksaon.kit@mahidol.ac.th
Cameron D. Haydinger: cameron.haydinger@adelaide.edu.au
John P.M. Wood: john.wood2@sa.gov.au
Teresa Mammone: teresa.mammone@adelaide.edu.au
Robert J. Casson: robert.casson@adelaide.edu.au
Daniel J. Peet: daniel.peet@adelaide.edu.au

Word count abstract: 204
Word count text: 5,418

Color should be used for all figures in print.

**Abstract**

Müller cells (MCs) play a crucial role in the retina, and cultured MC lines are an important tool with which to study MC function. Transformed MC lines have been widely used; however, the transformation process can also lead to unwanted changes compared to the primary cells from which they were derived. To provide an alternative experimental tool, a monoclonal novel spontaneously immortalized rat Müller cell line, SIRMu-1, was derived from primary rat MCs and characterized. Immunofluorescence, western blotting and RNA-sequencing demonstrate that the SIRMu-1 cell line retains similar characteristics to cultured primary MCs in terms of expression of the MC markers cellular retinaldehyde-binding protein, glutamine synthetase, S100, vimentin and glial fibrillary acidic protein at both the mRNA and protein levels. Both the cellular morphology and overall transcriptome of the SIRMu-1 cells are more similar to primary rat MCs than the commonly used rMC-1 cells, a well-described, transformed rat MC line. Furthermore, SIRMu-1 cells proliferate rapidly, have an effectively indefinite life span and a high transfection efficiency. The expression of Y chromosome specific genes confirmed that the SIRMu-1 cells are derived from male MCs. Thus, the SIRMu-1 cell line represents a valuable experimental tool to study roles of MCs in both physiologic and pathologic states.

**Keywords**: Müller cell; spontaneously immortalized cell; SIRMu-1; retina; cell culture

**List of abbreviations**

CMF-HBSS, calcium- and magnesium-free Hank’s balanced salt solution

cpm, count per million reads

CRALBP, cellular retinaldehyde-binding protein

DAPI, 4’,6-diamidino-2-phenylindole dihydrochloride

DEGs, differentially expressed genes

FBS, fetal bovine serum

FDR, false discovery rate

GFAP, glial fibrillary acidic protein

GO, gene ontology

GS, glutamine synthetase

HBSS, Hank’s balanced salt solution

HPV, human papillomavirus

MCs, Müller cells

MEM, minimal essential medium

mRNA-seq, mRNA sequencing

NG2, neuron glial antigen-2

PBS-HS, horse serum in phosphate-buffered saline

PEI, polyethylenimine

RPE, retinal pigmented epithelial

RPKM, reads per kilobase per million

SIRMu, spontaneously immortalized rat Müller cells

SIRMu-1, spontaneously immortalized rat Müller cell line

SV40, simian virus 40

## 1. Introduction

Müller cells (MCs) are the major type of glial cell of the vertebrate retina. They have diverse functions, including mechanical support of the neural retina, removal of neurotransmitters from the extracellular space, spatial buffering of potassium cations, storage of glycogen, and possible transfer of substrates for cellular metabolic reactions to neighboring neurons (Bringmann et al., 2006; Vecino et al., 2016). Since they span the entire thickness of the retina, MCs have also been proposed to guide light to photoreceptors in the inner retinal layer, reducing light scattering and increasing visual acuity (Franze et al., 2007; Labin and Ribak, 2010). Stressed MCs undergo gliosis and have been shown to dedifferentiate into multipotent progenitor cells which can subsequently differentiate into retinal neurons, including photoreceptors (Bringmann et al., 2006; Jadhav et al., 2009; Jayaram et al., 2014; Lawrence et al., 2007; Ramirez et al., 2012; Vecino et al., 2016). Experimental systems using cultured primary MCs enable detailed biochemical analysis of this important cell type, and allow chemical and genetic manipulation (Linser and Moscona, 1979; Sarthy, 1985; Savage et al., 1988). However, analysis of primary cells is restricted by difficulties in acquiring and maintaining the cells, slow proliferation rates, early senescence, and low transfection efficiency (Roque et al., 1997; Sarthy et al., 1998).

As an alternative to primary MCs, numerous studies use immortalized MCs, which proliferate rapidly, do not senesce and are relatively easy to maintain and manipulate. These immortalized MCs have been largely generated by transformation of primary cells with viral oncogenes. The rMC-1 and the RMC

HPV-16 E6/E7 rat MC lines, for example, were immortalized by transfecting primary MCs with simian virus 40 (SV40) DNA and by transducing with human papillomavirus (HPV) type 16 E6 and E7 viral construct, respectively (Roque et al., 1997; Sarthy et al., 1998). However, the transformation process can alter other characteristics in addition to proliferation and life span compared to primary cells, such as cellular morphology (Sarthy et al., 1998) and metabolism (Bissell et al., 1972). Hence, spontaneously immortalized cell lines which have not been intentionally transformed by exogenous reagents often retain a greater similarity to primary cells than transformed cells, and therefore serve as a more relevant experimental tools.

To provide an alternative and valuable model for MC research, we established and characterized a novel spontaneously immortalized rat Müller cell line, SIRMu-1. The MC-like characteristics of this monoclonal line are described in relation to primary rat MCs and the commonly-used transformed rat MC line rMC-1 (Sarthy et al., 1998), including cellular morphology, expression of MC and other retinal cell marker proteins, a comprehensive transcriptomic analysis and transfection efficiency.

## 2. Materials and Methods

### 2.1 Primary rat mixed retinal, MC and retinal pigmented epithelial (RPE) cell cultures

Sprague-Dawley rats were used for the generation of primary MC cultures. Handling of these animals conformed to the Australian Code of Practice for the Care and Use of Animals for Scientific Purposes 2004, and the ARVO

Statement for the Use of Animals in Ophthalmic and Vision Research. Mixed retinal cell cultures consisting of neurons, photoreceptors and glial cells were prepared from litters of 1-5 day post-natal pups using a trypsin-mechanical digest method as described previously (Wood et al., 2005; Wood et al., 2003). Briefly, freshly dissected rat pup retinas were incubated for 5 minutes in a shaking water bath in sterile incubation medium (5.4 mM KCl, 116 mM NaCl, 0.096 mM $NaH_2PO_4 \cdot 2H_2O$, 19.5 mM glucose, 0.15 mM $MgSO_4$, 23.8 mM $NaHCO_3$, 3 g/L bovine serum albumin, 10 mg/L phenol red) containing 0.1 mg/ml trypsin. After allowing tissue to settle for an additional 5 minutes, the trypsin/incubation medium was removed and replaced with incubation medium containing 1,000 U DNAse (bovine pancreas, type II), soybean trypsin inhibitor (type I-S, 0.667 mg/ml) and 0.19 mM $MgSO_4$. After a further 5 minutes, trituration was carried out with a flame-rounded glass pipette until all tissue had been dissociated. After a brief centrifugation (180 g / 5 minutes / 4 $^oC$) dissociated retinal cells were resuspended and then grown in minimal essential medium (MEM, +Earle's Salts, -L-glutamine, #11090, Life Technologies Australia, Scoresby, VIC, Australia) containing 10% fetal bovine serum (FBS), 87 mg/L gentamicin sulfate, 2.2 mg/L amphotericin B, 25 mM glucose and 2 mM L-glutamine. Cultures were maintained in a humidified incubator at 37$^oC$, 5% $CO_2$ without disruption for 7 days, and then continuously maintained with medium changed every 3 days for 28-42 days until almost all other cell types died and detached from the culture vessel surface, leaving predominantly MCs (Osborne, 1990; Wood et al., 2005). Once isolated, MC cultures were grown as above but with 20% FBS, and used at passage numbers 2-4 for experiments.

Production of primary RPE cell cultures was based on a method described previously (Mayerson et al., 1985). Litters of 10-12 day old Dark Agouti rat pups were used to generate cultures. Briefly, enucleated eyes from pups were washed in Hank's balanced salt solution (HBSS with 1.26 mM $CaCl_2$, 0.49 mM $MgCl_2.6H_2O$, 0.41 mM $MgSO4.7H_2O$, #14025-092, Life Technologies Australia), containing 50 µg/ml gentamicin and 100 µg/ml kanamycin. Intact eyes were subsequently incubated in HBSS containing 100 U/ml of collagenase and 50 U/ml hyaluronidase for 60 minutes followed by incubation in calcium- and magnesium-free HBSS (CMF-HBSS) containing 1 mg/ml trypsin for 60 minutes. Eyes were transferred to growth medium (MEM containing 2 mM L-glutamine, gentamicin/kanamycin as above, and 20% FBS), where they were opened via a circumferential incision immediately below the ora serrata and the anterior segment, and vitreous and retina were discarded. RPE sheets were brushed out of eye-cups in fresh growth medium, rinsed and incubated in CMF-HBSS containing 1 mg/ml trypsin for 5 minutes. RPE cells were mechanically dissociated, centrifuged (180 g / 5 minutes / 4 $^oC$) and adjusted to 1,000 cells/$mm^3$ in growth medium. Cultures were maintained in growth medium and were used at passage number 2 for experiments.

**2.2 Establishment of a spontaneously immortalized rat MC line and monoclonal isolation.**

Rapidly-proliferating, spontaneously immortalized cells were derived from primary MCs in a mixed retinal cell culture and cultured in MEM containing

20% FBS (unless otherwise stated), 25 mM glucose and 2 mM glutamine at 37ºC with 5% $CO_2$. A monoclonal line was isolated from these cells by 2 sequential rounds of single cell cloning by serial dilution. For each round, 4,000 cells were added to well A1 of a 96-well plate. Serial ½ dilutions were performed vertically down the first column on the plate (wells A1-A8). Each of these wells were then serially diluted ½ horizontally across the plate. Culture medium was added to each well to give a final volume of 200 µl, and plates incubated for 14-20 days. Single clones were selected as a single colony of growth at the highest dilutions across the plate. After 2 sequential rounds of single cell isolation 8 monoclonal lines were generated, all of which retained a similar morphology to primary MCs and a rapid proliferation. One was expanded and named the spontaneously immortalized rat Müller cell line SIRMu-1. SIRMu-1 cells of passage numbers 6-22 were used for experiments.

### 2.3 Culture of the rMC-1 cell line

The rMC-1 cells were a kind gift of Dr Vijay Sarthy (Northwestern University, Chicago, IL, USA), obtained from Dr Binoy Appukuttan (Flinders University, Adelaide, SA, Australia), and maintained under the same conditions as the SIRMu-1 line but with 10% FBS. Cells of passage numbers 23-34 were used for experiments.

### 2.4 Immunocytochemical analysis

Immunofluorescence was performed as previously described (Wood et al., 2012) with minor modifications as outlined below. Cells seeded on coverslips, coated with 0.2% gelatin in phosphate-buffered saline (PBS), were fixed with

4% paraformaldehyde/PBS for 20 minutes, washed with PBS, permeabilized by incubating in 0.1% triton X-100/PBS for 15 minutes at room temperature, washed with PBS, and blocked with 3.3% (v/v) horse serum/PBS (PBS-HS) for 15 minutes at room temperature. Primary antibody incubation was performed overnight at room temperature using antibodies diluted in PBS-HS against vimentin, SV40 T-antigen, S100, glial fibrillary acidic protein (GFAP), rhodopsin, blue cone opsin, tau, CD11b, neuron glial antigen-2 (NG2), and RPE65 (Table 1). The following day, cells were incubated for 1 hour at room temperature with secondary antibodies (1:250 to 1:500 dilutions; Life Technologies Australia): anti-mouse Alexa Fluor 594 (#A11005, #A21203), anti-rabbit Alexa Fluor 594 (#A21207), anti-rabbit Alexa Fluor 488 (#A21206), and anti-goat Alexa Fluor 594 (#A11058) antibodies. Nuclear counterstaining was performed with 500 ng/mL 4’,6-diamidino-2-phenylindole dihydrochloride (DAPI; #D8417, Sigma-Aldrich, Castle Hill, NSW, Australia). Cell coverslips were mounted onto glass slides with a fluorescence-protecting mounting medium (ProLong Gold Antifade Mountant, #P10144, Life Technologies Australia) and visualized using fluorescence microscopy (Nikon Eclipse Ti microscope, Nikon Australia, Rhodes, NSW, Australia).

### 2.5 Western blotting

Protein lysates were prepared in whole cell extract buffer (20 mM HEPES pH 7.8, 0.42 M NaCl, 0.5% Igepal, 25% glycerol, 0.2 mM EDTA, 1.5 mM $MgCl_2$ with freshly added 1 mM DTT, 1 mM PMSF, 2 µg/mL aprotinin, 4 µg/mL bestatin, 5 µg/mL leupeptin, and 1 µg/ml pepstatin), and quantified by Bio-rad protein assay (#5000006, Bio-Rad Laboratories, Gladesville, NSW, Australia).

Equivalent amounts of total protein were separated on 10% SDS-PAGE and transferred to nitrocellulose membranes using a Trans-Blot Turbo Transfer System (Bio-Rad Laboratories). Membranes were blocked with 10% (w/v) skimmed milk in PBS containing 0.1% nonionic detergent (TWEEN20, #P1379, Sigma-Aldrich) for 1 hour at room temperature, incubated overnight at 4$^{o}$C with primary antibodies for glutamine synthetase (GS), cellular retinaldehyde-binding protein (CRALBP), and $\alpha$-tubulin (Table 1) diluted in 2% skimmed milk in 0.1%TWEEN20/PBS, and detected using horseradish peroxidase-conjugated secondary antibodies (goat anti-mouse IgG, #31430, Life Technologies Australia, and goat anti-rat IgG, #ab6845, Abcam, Melbourne, VIC, Australia; both at 1:5000 dilution) and visualized using chemiluminescence and a Bio-Rad ChemiDoc Imaging system (Bio-Rad Laboratories).

**2.6 mRNA sequencing (mRNA-seq)**

Primary MCs, SIRMu-1 and rMC-1 cells were trypsinised, pelleted and RNA extracted with a *mir*Vana miRNA Isolation Kit (#AM1561, Life Technologies Australia). RNA samples (4 biological replicates of primary MCs of passage numbers 3-4, 5 of SIRMu-1 cells of passage numbers 6-20, and 3 of rMC-1 cells of passage numbers 23-26) were submitted to the Australian Cancer Research Foundation (ACRF) Cancer Genomics Facility (Adelaide, SA, Australia), quality determined with an Agilent RNA 6000 Nano kit (#5067-1511, Agilent Technologies, Santa Clara, CA, USA) on an Agilent 2100 bioanalyzer and concentrations determined using a Qubit RNA HS assay kit (#Q32852, Life Technologies Australia). 5 ng of enriched polyA RNA was used for library

preparation by a KAPA stranded RNAseq HyperPrep kit (#KK8544, KAPA, Cape Town, South Africa). Briefly, RNA was fragmented (approximate insert length: 200 basepairs) and converted to cDNA, followed by end-repair and A-tailing. Adapters compatible with Illumina sequencing were ligated to the cDNA with an approximate adapter to molar insert ratio of 200:1, and a post-ligation clean-up to remove excess adapters performed. The libraries were amplified with 10 cycles of PCR and cleaned with 1X ratio of beads. Library sizes and yields were confirmed using an Agilent High Sensitivity DNA kit (#5067-4626, Agilent Technologies) with an Agilent 2100 bioanalyzer and diluted to 4 nM stocks. Libraries were pooled in equimolar ratios and sequenced on an Illumina NextSeq 500 system using a 75 cycle high output kit (#FC-404-2005, Illumina, San Diego, CA, USA).

### 2.7 Analysis of mRNA-seq data

Sequencing reads were mapped to the reference rat genome (Rnor_6.0) using the STAR algorithm (Dobin et al., 2013). Raw count data were imported into R. Genes that were either not expressed or expressed at very low levels (not detected at greater than one count per million reads (cpm) for all samples of at least one group) were filtered out of the analysis. Counts for the remaining genes (10,236 genes) were normalised to library size and composition using the “TMM” method in Bioconductor’s EdgeR package (McCarthy et al., 2012; Robinson et al., 2010). The TMM normalised data were used for generation of the multidimensional scaling plot.

Differential expression was determined using Bioconductor's Limma package which employs a linear modelling approach (Ritchie et al., 2015). A fold-change threshold of 5 with a Benjamini-Hochberg corrected P-value of < 0.05 defined whether a gene was differentially expressed (Benjamini and Hochberg, 1995). Gene ontology (GO) analysis was also performed. Overrepresentation of GO-slim biological process terms (PANTHER annotation version 13.1, released 2018-02-03) among lists of differentially expressed genes, relative to the *Rattus norvegicus* reference list, was assessed using the PANTHER statistical overrepresentation test (released 2017-12-05) (Mi et al., 2017). Fisher's exact test with false discovery rate (FDR) correction was used, and terms with a FDR < 0.05 were considered overrepresented.

For generation of the heatmap showing expression of MC marker genes, TMM normalised count data were further normalised to transcript length (downloaded from the Ensembl database, release 91 (Zerbino et al., 2018), Rnor_6.0, INSDC Assembly GCA_000001895.4) to obtain reads per kilobase per million (RPKM) for each gene, and log-transformed by taking $\log_2$(RPKM + 1).

### 2.8 Transfection efficiency

SIRMu-1 and rMC-1 cells were seeded into a 24-well plate (20,000 cells per well), and transfected 20-24 hours later with a plasmid encoding nuclear Tomato fluorescence protein (500 ng per well) using either FuGENE HD (#E2311, Promega Australia, Alexandria, NSW, Australia), FuGENE 6

(#E2692, Promega Australia), Lipofectamine 2000 (#11668019, Life Technologies Australia) or Polyethylenimine (PEI) (#23966-1, Polysciences, Warrington, PA, USA) according to the manufacturers' instructions, at a transfection reagent:DNA ratio of 3:1. 24 hours after transfection the cells were labelled with Hoechst 33342 nuclear stain (NucBlue Live ReadyProbes Reagent, #R37605, Life Technologies Australia) and imaged using fluorescence microscopy (Nikon Eclipse Ti microscope, Nikon Australia). Transfection efficiency was calculated from proportions of Tomato fluorescence-positive transfected cells to total cell numbers indicated by nuclear staining. Cell counts were performed on three different fields of vision for each sample using the Fiji (a distribution of ImageJ) software (Schindelin et al., 2012). Data are presented as mean ± SD of 3 independent experiments.

## 3. Results

### 3.1 Establishment and initial characterization of spontaneously immortalized Rat Müller Cells

Primary MC cultures were generated by continuous culturing for 28-42 days of mixed retinal cells derived from rat neonatal retinas, resulting in the loss of retinal neurons and other cell types to leave an almost homogeneous population of MCs (Osborne, 1990; Wood et al., 2005). The cultured primary MCs were typically large, flat and adherent with a unique "ghost-like" morphology, and a large nucleus (Fig. 1A) (Roque et al., 1997; Sarthy, 1985; Sarthy et al., 1998; Vecino et al., 2016; Wood et al., 2005). Primary rat MCs proliferate with a doubling time of approximately 7 days and typically senesce after 4 to 8 divisions.

After 28 days of culturing a batch of neonatal rat mixed retinal cells, a visible colony of rapidly-proliferating cells was observed. These large cells had a similar morphology to primary MCs (Fig. 1A). The proliferating cells were passaged and continued to rapidly proliferate beyond 12 weeks, well after the time which primary MCs would typically senesce (Sarthy, 1985). The doubling time of these cells was approximately 2-3 days, and they retained a MC-like morphology. As these cells had survived for more than 12 weeks *in vitro*, had been derived under the commonly-used conditions to generate primary MC cultures and had a characteristic morphology of MCs, it was hypothesized that they originated from primary MCs, and not another retinal cell type. These cells were maintained in culture, being passaged at 1:10 every 5-7 days. After 30 passages (approximately 7 months) these cells still proliferated rapidly and maintained a morphology similar to primary MCs (data not shown). Arising from primary cultures without having been transformed, they were named spontaneously immortalized rat Müller cells (SIRMu).

Initial characterization was performed on early passage number cells (passage number 6) to confirm that these SIRMu cells display common features of MCs. Analysis by immunocytochemistry clearly shows that the MC marker vimentin is expressed in the cytoplasm of every cell, similar to primary MCs and the transformed rMC-1 cell line (Fig. 1B). Since the SIRMu cells were established while the transformed rMC-1 cells were being cultured in the same facility, it was important to confirm that the SIRMu cells were unique, and not simply a potential contamination of primary MCs with rMC-1 cells, although the smaller,

more elongated and spindle-like morphology of the rMC-1 cells (Fig. 1A) indicated that such a contamination was unlikely. Hence, the SIRMu cells were labelled for expression of the SV40 T-antigen used to generate the rMC-1 cells (Sarthy et al., 1998). Figure 1C shows that as expected the rMC-1 cells label strongly for the nuclear SV40 T-antigen, while both the primary MCs and the SIRMu cells do not show any staining, demonstrating that the SIRMu cells are a unique line of spontaneously immortalized cells. These SIRMu cells have now been continuously cultured for more than 32 months and passaged over 140 times (greater than 400 population doublings), consistent with effectively indefinite growth (Pirisi et al., 1987; Roque et al., 1997).

### 3.2 Monoclonal isolation of the SIRMu cells

To ensure purity of this spontaneously immortalized line, we generated a single monoclonal line by performing 2 sequential rounds of cell cloning by serial dilution on the SIRMu cells (from passage 9 of the original preparation). The first passage after the first serial dilution was defined as passage number 1 for the isolated monoclonal line. This monoclonal line had a similar proliferation rate and morphology to the original culture, and was named SIRMu-1. Immunocytochemistry demonstrated that the monoclonal SIRMu-1 cells do not express the SV40 T-antigen and hence were not derived from rMC-1 cells (Fig. 1C).

The SIRMu-1 cell line has been cultured in both 10% and 20% FBS, with estimated doubling times of 36 and 30 hours, respectively. To date, it has

been passaged over 40 times and has retained a similar morphology to primary MCs.

### 3.3 Marker protein expression of the SIRMu-1 cells

To validate that the SIRMu-1 cells were derived from MCs, immunocytochemistry was performed on primary MCs, SIRMu-1 and rMC-1 cells to detect expression of the commonly used MC markers vimentin and S100, in addition to the glial cell marker GFAP (Lewis et al., 1988; Limb et al., 2002; Roque et al., 1997; Sarthy et al., 1998) (Fig. 1B, 2A, 2B). The SIRMu-1 cells express all of these markers at similar levels to the primary MCs and the rMC-1 cells. Western blotting analysis of two other MC markers, GS (Linser and Moscona, 1979; Sarthy, 1985) and CRALBP (Bunt-Milam and Saari, 1983; Sarthy et al., 1998) (Fig. 2D) show that both the SIRMu-1 and the rMC-1 cells express GS, but at a lower level compared to primary MCs, and that all 3 cell lines express a low level of CRALBP.

In addition to MCs, other retinal cell types can be present in mixed retinal cultures, including rod and cone photoreceptors, neurons, astrocytes, microglia, pericytes, and RPE cells (Wood et al., 2005; Wood et al., 2012). To confirm that the SIRMu-1 cells were not derived from other non-MC cell types, immunofluorescence was performed for expression of rhodopsin (a marker of rod photoreceptors), blue cone opsin (cone photoreceptors), tau (neurons), CD11b (microglia), NG2 (pericytes), and RPE65 (RPE cells) (Fig. 3). In contrast to mixed retinal cultures, in which distinct populations of cells positively label for rhodopsin, blue cone opsin, tau, CD11b and NG2, the

SIRMu-1 cells do not show expression of any of these markers, with the exception of NG2 where low levels of staining slightly above background are visible (Fig. 3A-E). As expected, cultured primary rat RPE cells express RPE65, while the SIRMu-1 cells do not (Fig. 3I). Finally, although rat retinal astrocytes can also be immunoreactive to vimentin, S-100, GFAP and GS (Derouiche and Rauen, 1995; Mansour et al., 2008; Vecino et al., 2016), in culture they have a characteristic star shape with a smaller nucleus (Vecino et al., 2016) that is distinct from primary MCs and the SIRMu-1 cells, and they do not express the MC-specific marker CRALBP observed in the SIRMu-1 cells (Fig. 2D). Hence, it is clear that the SIRMu-1 were not derived from astrocytes. Taken together these data strongly support the hypothesis that the SIRMu-1 cells originated from primary MCs rather than any other retinal cell type, and that they retain MC-like characteristics, including their distinct morphology and the expression of MC marker proteins.

### 3.4 Transcriptomic analysis of the SIRMu-1, primary MCs, and the rMC-1

To further characterize the SIRMu-1 cell line, the transcriptomes of the SIRMu-1, primary MCs and rMC-1 cells were analysed using mRNA-seq. RNA was isolated from 5 biological replicates of SIRMu-1 cells, 4 of primary MCs, and 3 of the rMC-1. To control for potential differences in gene expression between cell types being due to differences in culture media, 2 out of the 5 SIRMu-1 RNA samples were isolated from cells grown in the presence of the antibiotic gentamicin and the antifungal amphotericin B, to match the culture conditions of the primary MCs, whereas the other 3 samples were isolated from SIRMu-1 cells grown in the absence of these drugs, which is the usual culture condition

of SIRMu-1 and rMC-1 cells. The total RNA was polyA enriched, barcoded and sequenced, with 44-84 million reads per sample (60 million average). Transcripts from 10,236 different genes were detected at significant levels in all cells.

Analysis of the sequences obtained showed that on average 98.25% of reads per sample (range of 97.91-98.47%) mapped successfully to the rat genome, confirming that all three lines are of rat origin. Based on overall gene expression, a multidimensional scaling plot shows clustering of the RNA-seq samples (Fig. 4A). Three distinct clusters of samples are evident, each representing one of the distinct cell types, indicating that the sequencing results were consistent among replicates within the same cell groups. Importantly, the multidimensional scaling plot demonstrates that the transcriptome of the SIRMu-1 cells is more similar to the transcriptome of the primary MCs than the rMC-1 transcriptome is to the primary MCs. These data also demonstrate that there are no large differences in gene expression profiles between all of the 5 SIRMu-1 samples, including the 2 samples derived from cells cultured in medium with gentamicin and amphotericin B, indicating that the two drugs in the growth medium do not have a major effect on the transcriptome.

Transcriptomic differences between groups were further examined by comparing differentially expressed genes (DEGs) between each of the two immortalized cell lines and the primary MCs. Genes that were expressed at very low levels or not expressed in all groups were first filtered out of the

analysis, leaving 10,236 genes that were tested for differential expression. Genes that were upregulated or downregulated greater than 5-fold compared to the primary MCs were considered differentially expressed. A total of 10,036 genes (98% of the 10,236 expressed genes) were not differentially expressed in the SIRMu-1 cell line compared to the primary MCs, with 200 genes differentially expressed. Among these 200 DEGs, 13 genes were upregulated and 187 were downregulated (Fig. 4B). In comparison, for the rMC-1 cells 9,304 genes (91%) were not differentially expressed compared to the primary MCs, but 932 genes were, with 314 upregulated and 618 downregulated (Fig. 4B). These data indicate that both the SIRMu-1 and rMC-1 cell lines have a similar transcriptome to the primary MCs, but that the SIRMu-1 cells are more closely related to the primary MCs than are the rMC-1 cells.

Interestingly, among the 200 DEGs in the SIRMu-1 compared to primary MCs and the 932 DEGs in the rMC-1 compared to primary MCs, there were 126 genes in common (Supplementary fig. S1A, supplementary tables S1). For the remainder of the DEGs, 74 genes are differentially expressed uniquely in the SIRMu-1 cells, while 806 genes were differentially expressed uniquely in the rMC-1 cells (Supplementary fig. S1A, supplementary tables S1). To assess functional differences between each immortalized cell line and primary MCs, GO analyses were performed using the PANTHER classification system. The lists of genes differentially expressed in both cell lines with respect to primary MCs were classified by GO-Slim biological process terms, and statistically overrepresented terms were determined by comparison to their frequency in a reference rat genome. There were no statistically significantly (FDR < 0.05)

overrepresented biological process terms among the 74 genes differentially expressed between SIRMu-1s and primary MCs, nor among the 126 genes differentially expressed in both cell lines compared to primary MCs, possibly due in part to the relatively low number of genes in these two groups. However, there was significant overrepresentation of terms among the 806 genes differentially expressed between rMC-1s and primary MCs. The top 10 such terms by fold-enrichment are shown in supplementary figure S1B. Consistent with being a highly-proliferative transformed cell line, a large proportion of the DEGs in rMC-1 cells are involved in DNA replication and cell division-related processes.

Next, expression of the transcripts encoding the MC marker proteins were examined. The SIRMu-1 cells express similar levels of transcripts encoding vimentin, S100, and GFAP to the primary MCs and rMC-1 cells, with transcripts encoding GFAP expressed at low levels (Fig. 4C). SIRMu-1 and rMC-1 cells also express GS transcripts, but at a lower level compared to the primary MCs. All cell types express CRALBP transcripts at very low levels with an average of 0.06, 0.15, and 1.16 cpm in primary MCs, SIRMu-1 and rMC-1 cells, respectively. These results are consistent with protein expression from immunocytochemical and western blotting analyses (Fig. 1 and 2). Furthermore, SIRMu-1 and rMC-1 cells express very low to undetectable levels of transcripts encoding rhodopsin, blue cone opsin, tau, CD11b, and RPE65, markers used in the immunofluorescence analysis that are characteristic of other retinal cell types including rod and cone photoreceptors, neurons, microglia, and RPE cells (Fig. 3). Of note, while SIRMu-1 cells

express transcripts encoding NG2, a pericyte marker, the levels are many fold lower than the vimentin transcripts in these cells (Fig. 4C), and primary MCs and rMC-1 cells also express NG2 at low levels. Together these data show that the SIRMu-1 cells display a MC-like transcriptomic profile, and also authenticate the MC characteristics of the rMC-1 cells used in the present study.

Finally, we examined the expression of gender-specific genes between the three different MC types. Compared to primary MCs, which were derived from mixed litters presumed to contain both male and female pups, the SIRMu-1 cells show an upregulation of two Y chromosome-specific genes, *Eif2s3y* and *Ddx3*, consistent with the SIRMu-1 cell line originating from a male pup. In contrast, *Eif2s3y* and *Ddx3* were not expressed at significant levels in the rMC-1 cell samples, nor were any other Y chromosome-specific genes, consistent with rMC-1 cell line being derived from a female rat.

### 3.5 Transfection efficiency

One key advantage of most immortalized cell lines is high transfection efficiency with standard transfection reagents, such as cationic lipids, compared to primary cells. To determine transfection efficiency of the SIRMu-1 cell line, various commercially-available lipid-based transfection reagents were used to transfect SIRMu-1 cells with a fluorescence reporter gene, and transfection efficiency was measured using fluorescence microscopy (Table 2). The transfection efficiency of the SIRMu-1 cells is between 7 and 14%, which is similar to that achieved with the rMC-1 cells (6-24%), and

approximately 10-fold higher than what we observed with the primary MCs (1.9%).

## 4. Discussion

Immortalized rat MC lines generated via transformation, such as rMC-1 (Sarthy et al., 1998), RMC HPV-16 E6/E7 (Roque et al., 1997) and TR-MUL5 (Tomi et al., 2003), have been used extensively for the analysis of MC function. Similar to the spontaneously immortalized human MC line MIO-M1 (Limb et al., 2002) and the spontaneously immortalized murine MC line QMMuC-1 (Augustine et al., 2018) serving as an alternative model for studying human and mouse MCs, respectively, the spontaneously immortalized SIRMu-1 cells described here provide an alternative system for investigating MC function in rat cells not transformed with viral oncogenes. Although the mechanism of spontaneous immortalization remains to be ascertained, the SIRMu-1 cells appear capable of proliferating indefinitely.

SIRMu-1 cells, like transformed rMC-1 cells, display key characteristics of primary MCs, including the expression of an array of well-characterized MC marker proteins (Fig. 1B and 2) and genes (Fig. 4C). The presence of transcripts encoding the MC markers vimentin, GS and CRALBP (Fig. 4C) in all 3 types of MCs investigated in the present study is consistent with published reports on rat and mouse MC transcriptomes (Roesch et al., 2008; Ueno et al., 2017; Zhao et al., 2015). Furthermore, the lack of expression of key markers indicative of other major retinal cell types (Fig. 3) supports the conclusion that SIRMu-1 cells were derived from primary MCs.

While most MC markers were expressed at similar levels when comparing the two immortalized lines and the primary MCs, at both the mRNA and protein levels, the SIRMu-1 and the rMC-1 cell lines express GS at a lower level than the primary MCs (Fig. 2D and 4C). GS catalyzes the conversion of glutamate to glutamine in MCs, playing an important role in the neurotransmitter recycling process, an essential function of MCs in support of retinal neurons (Bringmann et al., 2006; Vecino et al., 2016). The decreased GS expression levels may reflect changes due to extended propagation in culture in the absence of retinal neurons, consistent with previous studies (Germer et al., 1997; Hauck et al., 2003; Lewis et al., 1999; Lewis et al., 1989; Roque et al., 1997). Similarly, this may also explain the low expression levels of the MC marker CRALBP in all 3 types of MCs investigated (Fig. 2D). CRALBP in MCs *in vivo* is involved in the recycling of photopigments derived from photoreceptors (Das et al., 1992); the absence of functional light-sensitive photoreceptors and prolonged culture likely leads to a decrease in CRALBP expression (Hauck et al., 2003; Lewis et al., 1989; Pfeffer et al., 2016). In addition, our finding that the cultured MCs express GFAP (Fig. 2B and 4C) is consistent with a number of published studies (Limb et al., 2002; Roque et al., 1997; Sarthy et al., 1998).

Overall, the transcriptome of the SIRMu-1 cells closely resembles the transcriptome of primary MCs. The rMC-1 cells are also transcriptomically similar to the primary MCs but to a lesser degree than are the SIRMu-1 cells. While the rMC-1 cells do have a greater number of genes showing differential

expression when compared to the primary MCs than the SIRMu-1 cells (Fig. 4B), this may be in part a function of the more consistent gene expression profiles among the independent rMC-1 samples (revealed in the close clustering for rMC-1 samples in Fig. 4A). Not surprisingly, genes encoding proteins involved in DNA replication and cell cycle/division were overrepresented in the rapidly-proliferating rMC-1 transcriptomes compared to the primary MCs (Supplementary fig. S1B). In contrast, DNA replication and cell cycle/division were not overrepresented in the list of genes differentially expressed between the rapidly-proliferating SIRMu-1 cells and the primary MCs, even when the stringency of differential expression was reduced to 2-fold (data not shown). This may reflect differences between transformation with viral oncogenes and the spontaneous immortalization observed here on cell proliferation, or it may be that a transcriptomic analysis of more SIRMu-1 samples is required to detect significant changes in expression of genes contributing to cellular proliferation. Furthermore, the rMC-1s cells were derived from adult rats (Sarthy et al., 1998) which may contribute to the bigger transcriptomic differences observed here between these cells and the primary neonatal rat MCs used in this study, compared to between the SIRMu-1 and the primary MCs. It is important to note, however, that the SIRMu-1 cells retaining the distinct large, flat, ghost-like shape are morphologically similar to both cultured primary adult rat MCs (Roque et al., 1997; Sarthy, 1985; Sarthy et al., 1998) and cultured primary neonatal rat MCs (Wood et al., 2005) (Fig. 1A), in contrast to the smaller, fibroblast-like morphology of the rMC-1 cells (Sarthy et al., 1998) (Fig. 1A). Given the well-established sex-related differences in retinal function (Chaychi et al., 2015; Wagner et al., 2008), the

male genotype of the SIRMu-1 cells compared to the female genotype of rMC-1 cells also represents another important difference. It is also noteworthy that while the SIRMu-1 cells are transcriptomically and morphologically similar to primary MCs, other metabolic or functional properties of these cells are not compared.

In summary, we present the establishment and characterization of the SIRMu-1 cell line, which to our knowledge is the first spontaneously immortalized cell line derived from primary rat MCs. SIRMu-1 cells display similar morphology and gene expression profiles to primary MCs, but proliferate more rapidly, have an effectively indefinite life span, and are more amenable to transfection. Thus, these SIRMu-1 cells comprise a valuable new tool for investigation of MC function and roles in retinal health and disease.

**Acknowledgements**

The authors thank Joel Geoghegan, Andreas Schreiber, Wendy Parker and Ming Lin (ACRF Cancer Genomics Facility, Adelaide, SA, Australia) for their assistance with the RNA-seq, and members of the Peet and Whitelaw laboratories and Onruedee Khantisitthiporn (University of Adelaide, SA, Australia) for helpful discussion and technical assistance.

**Funding**

This work was supported by a project grant from the National Health and Medical Research Council of Australia (109932). The funding source has no involvement in the conduct of experiments, data analysis and interpretation,

the preparation of the manuscript and the decision to submit the work for publication

## Author contributions

T.K. conceived the project, planned experiments, carried out experimental work, interpreted the results, and wrote the paper. C.D.H. planned experiments, interpreted the results, and wrote the paper. J.P.M.W. planned experiments, provided primary cell cultures, carried out experimental work, interpreted the results, and edited the paper. T.M. provided primary cell cultures, and edited the paper. R.J.C. and D.J.P. conceived and supervised the project, planned experiments, interpreted the results, and edited the paper.

## References

Augustine, J., Pavlou, S., O'Hare, M., Harkin, K., Stitt, A., Curtis, T., Xu, H., Chen, M., 2018. Characterization of a Spontaneously Immortalized Murine Muller Glial Cell Line QMMuC-1. Investigative ophthalmology & visual science 59, 1666-1674.

Benjamini, Y., Hochberg, Y., 1995. Controlling the False Discovery Rate: A Practical and Powerful Approach to Multiple Testing. Journal of the Royal Statistical Society. Series B (Methodological) 57, 289-300.

Bissell, M.J., Hatie, C., Rubin, H., 1972. Patterns of glucose metabolism in normal and virus-transformed chick cells in tissue culture. Journal of the National Cancer Institute 49, 555-565.

Bringmann, A., Pannicke, T., Grosche, J., Francke, M., Wiedemann, P., Skatchkov, S.N., Osborne, N.N., Reichenbach, A., 2006. Muller cells in the healthy and diseased retina. Progress in retinal and eye research 25, 397-424.

Bunt-Milam, A.H., Saari, J.C., 1983. Immunocytochemical localization of two retinoid-binding proteins in vertebrate retina. The Journal of cell biology 97, 703-712.

Chaychi, S., Polosa, A., Lachapelle, P., 2015. Differences in Retinal Structure and Function between Aging Male and Female Sprague-Dawley Rats are Strongly Influenced by the Estrus Cycle. PloS one 10, e0136056.

Das, S.R., Bhardwaj, N., Kjeldbye, H., Gouras, P., 1992. Muller cells of chicken retina synthesize 11-cis-retinol. The Biochemical journal 285 ( Pt 3), 907-913.

Derouiche, A., Rauen, T., 1995. Coincidence of L-glutamate/L-aspartate transporter (GLAST) and glutamine synthetase (GS) immunoreactions in retinal glia: evidence for coupling of GLAST and GS in transmitter clearance. J Neurosci Res 42, 131-143.

Dobin, A., Davis, C.A., Schlesinger, F., Drenkow, J., Zaleski, C., Jha, S., Batut, P., Chaisson, M., Gingeras, T.R., 2013. STAR: ultrafast universal RNA-seq aligner. Bioinformatics 29, 15-21.

Franze, K., Grosche, J., Skatchkov, S.N., Schinkinger, S., Foja, C., Schild, D., Uckermann, O., Travis, K., Reichenbach, A., Guck, J., 2007. Muller cells are living optical fibers in the vertebrate retina. Proceedings of the National Academy of Sciences of the United States of America 104, 8287-8292.

Germer, A., Jahnke, C., Mack, A., Enzmann, V., Reichenbach, A., 1997. Modification of glutamine synthetase expression by mammalian Muller (glial) cells in retinal organ cultures. Neuroreport 8, 3067-3072.

Hauck, S.M., Suppmann, S., Ueffing, M., 2003. Proteomic profiling of primary retinal Muller glia cells reveals a shift in expression patterns upon adaptation to in vitro conditions. Glia 44, 251-263.

Jadhav, A.P., Roesch, K., Cepko, C.L., 2009. Development and neurogenic potential of Muller glial cells in the vertebrate retina. Progress in retinal and eye research 28, 249-262.

Jayaram, H., Jones, M.F., Eastlake, K., Cottrill, P.B., Becker, S., Wiseman, J., Khaw, P.T., Limb, G.A., 2014. Transplantation of photoreceptors derived from human Muller glia restore rod function in the P23H rat. Stem Cells Transl Med 3, 323-333.

Labin, A.M., Ribak, E.N., 2010. Retinal glial cells enhance human vision acuity. Phys Rev Lett 104, 158102.

Lawrence, J.M., Singhal, S., Bhatia, B., Keegan, D.J., Reh, T.A., Luthert, P.J., Khaw, P.T., Limb, G.A., 2007. MIO-M1 cells and similar muller glial cell lines derived from adult human retina exhibit neural stem cell characteristics. Stem Cells 25, 2033-2043.

Lewis, G., Mervin, K., Valter, K., Maslim, J., Kappel, P.J., Stone, J., Fisher, S., 1999. Limiting the proliferation and reactivity of retinal Muller cells during experimental retinal detachment: the value of oxygen supplementation. American journal of ophthalmology 128, 165-172.

Lewis, G.P., Erickson, P.A., Guerin, C.J., Anderson, D.H., Fisher, S.K., 1989. Changes in the expression of specific Muller cell proteins during long-term retinal detachment. Experimental eye research 49, 93-111.

Lewis, G.P., Kaska, D.D., Vaughan, D.K., Fisher, S.K., 1988. An immunocytochemical study of cat retinal Muller cells in culture. Experimental eye research 47, 855-868.

Limb, G.A., Salt, T.E., Munro, P.M., Moss, S.E., Khaw, P.T., 2002. In vitro characterization of a spontaneously immortalized human Muller cell line (MIO-M1). Investigative ophthalmology & visual science 43, 864-869.

Linser, P., Moscona, A.A., 1979. Induction of glutamine synthetase in embryonic neural retina: localization in Muller fibers and dependence on cell interactions. Proceedings of the National Academy of Sciences of the United States of America 76, 6476-6480.

Mansour, H., Chamberlain, C.G., Weible, M.W., 2nd, Hughes, S., Chu, Y., Chan-Ling, T., 2008. Aging-related changes in astrocytes in the rat retina: imbalance between cell proliferation and cell death reduces astrocyte availability. Aging Cell 7, 526-540.

Mayerson, P.L., Hall, M.O., Clark, V., Abrams, T., 1985. An improved method for isolation and culture of rat retinal pigment epithelial cells. Investigative ophthalmology & visual science 26, 1599-1609.

McCarthy, D.J., Chen, Y., Smyth, G.K., 2012. Differential expression analysis of multifactor RNA-Seq experiments with respect to biological variation. Nucleic Acids Res 40, 4288-4297.

Mi, H., Huang, X., Muruganujan, A., Tang, H., Mills, C., Kang, D., Thomas, P.D., 2017. PANTHER version 11: expanded annotation data from Gene Ontology and Reactome pathways, and data analysis tool enhancements. Nucleic Acids Res 45, D183-D189.

Osborne, N.N., 1990. Stimulatory and inhibitory actions of excitatory amino acids on inositol phospholipid metabolism in rabbit retina. Evidence for a specific quisqualate receptor subtype associated with neurones. Experimental eye research 50, 397-405.

Pfeffer, B.A., Xu, L., Porter, N.A., Rao, S.R., Fliesler, S.J., 2016. Differential cytotoxic effects of 7-dehydrocholesterol-derived oxysterols on cultured retina-derived cells: Dependence on sterol structure, cell type, and density. Experimental eye research 145, 297-316.

Pirisi, L., Yasumoto, S., Feller, M., Doniger, J., DiPaolo, J.A., 1987. Transformation of human fibroblasts and keratinocytes with human papillomavirus type 16 DNA. J Virol 61, 1061-1066.

Ramirez, M., Hernandez-Montoya, J., Sanchez-Serrano, S.L., Ordaz, B., Ferraro, S., Quintero, H., Pena-Ortega, F., Lamas, M., 2012. GABA-mediated induction of early neuronal markers expression in postnatal rat progenitor cells in culture. Neuroscience 224, 210-222.

Ritchie, M.E., Phipson, B., Wu, D., Hu, Y., Law, C.W., Shi, W., Smyth, G.K., 2015. limma powers differential expression analyses for RNA-sequencing and microarray studies. Nucleic Acids Res 43, e47.

Robinson, M.D., McCarthy, D.J., Smyth, G.K., 2010. edgeR: a Bioconductor package for differential expression analysis of digital gene expression data. Bioinformatics 26, 139-140.

Roesch, K., Jadhav, A.P., Trimarchi, J.M., Stadler, M.B., Roska, B., Sun, B.B., Cepko, C.L., 2008. The transcriptome of retinal Muller glial cells. The Journal of comparative neurology 509, 225-238.

Roque, R.S., Agarwal, N., Wordinger, R.J., Brun, A.M., Xue, Y., Huang, L.C., Nguyen, L.P., Shay, J.W., 1997. Human papillomavirus-16 E6/E7 transfected retinal cell line expresses the Muller cell phenotype. Experimental eye research 64, 519-527.

Sarthy, P.V., 1985. Establishment of Muller cell cultures from adult rat retina. Brain research 337, 138-141.

Sarthy, V.P., Brodjian, S.J., Dutt, K., Kennedy, B.N., French, R.P., Crabb, J.W., 1998. Establishment and characterization of a retinal Muller cell line. Investigative ophthalmology & visual science 39, 212-216.

Savage, F.J., Day, J.E., Hogg, P., Grierson, I., 1988. Tissue culture of retinal glial cells. Eye 2 Suppl, S164-179.

Schindelin, J., Arganda-Carreras, I., Frise, E., Kaynig, V., Longair, M., Pietzsch, T., Preibisch, S., Rueden, C., Saalfeld, S., Schmid, B., Tinevez, J.Y., White, D.J., Hartenstein, V., Eliceiri, K., Tomancak, P., Cardona, A., 2012. Fiji: an open-source platform for biological-image analysis. Nat Methods 9, 676-682.

Tomi, M., Funaki, T., Abukawa, H., Katayama, K., Kondo, T., Ohtsuki, S., Ueda, M., Obinata, M., Terasaki, T., Hosoya, K., 2003. Expression and regulation of L-cystine transporter, system xc-, in the newly developed rat retinal Muller cell line (TR-MUL). Glia 43, 208-217.

Ueno, K., Iwagawa, T., Ochiai, G., Koso, H., Nakauchi, H., Nagasaki, M., Suzuki, Y., Watanabe, S., 2017. Analysis of Muller glia specific genes and their histone modification using Hes1-promoter driven EGFP expressing mouse. Sci Rep 7, 3578.

Vecino, E., Rodriguez, F.D., Ruzafa, N., Pereiro, X., Sharma, S.C., 2016. Glia-neuron interactions in the mammalian retina. Progress in retinal and eye research 51, 1-40.

Wagner, H., Fink, B.A., Zadnik, K., 2008. Sex- and gender-based differences in healthy and diseased eyes. Optometry 79, 636-652.

Wood, J.P., Chidlow, G., Graham, M., Osborne, N.N., 2005. Energy substrate requirements for survival of rat retinal cells in culture: the importance of glucose and monocarboxylates. Journal of neurochemistry 93, 686-697.

Wood, J.P., Mammone, T., Chidlow, G., Greenwell, T., Casson, R.J., 2012. Mitochondrial inhibition in rat retinal cell cultures as a model of metabolic compromise: mechanisms of injury and neuroprotection. Investigative ophthalmology & visual science 53, 4897-4909.

Wood, J.P., Schmidt, K.G., Melena, J., Chidlow, G., Allmeier, H., Osborne, N.N., 2003. The beta-adrenoceptor antagonists metipranolol and timolol are retinal neuroprotectants: comparison with betaxolol. Experimental eye research 76, 505-516.

Zerbino, D.R., Achuthan, P., Akanni, W., Amode, M R., Barrell, D., Bhai, J., Billis, K., Cummins, C., Gall, A., Girón, C.G., Gil, L., Gordon, L., Haggerty, L., Haskell, E., Hourlier, T., Izuogu, O.G., Janacek, S.H., Juettemann, T., To, J.K., Laird, M.R., Lavidas, I., Liu, Z., Loveland, J.E., Maurel, T., McLaren, W., Moore, B., Mudge, J., Murphy, D.N., Newman, V., Nuhn, M., Ogeh, D., Ong, C.K., Parker, A., Patricio, M., Riat, H.S., Schuilenburg, H., Sheppard, D., Sparrow, H., Taylor, K., Thormann, A., Vullo, A., Walts, B., Zadissa, A., Frankish, A., Hunt, S.E., Kostadima, M., Langridge, N., Martin, F.J., Muffato, M., Perry, E., Ruffier, M., Staines, D.M., Trevanion, S.J., Aken, B.L., Cunningham, F., Yates, A., Flicek, P., 2018. Ensembl 2018. Nucleic Acids Research 46, D754-D761.

Zhao, M., Andrieu-Soler, C., Kowalczuk, L., Paz Cortes, M., Berdugo, M., Dernigoghossian, M., Halili, F., Jeanny, J.C., Goldenberg, B., Savoldelli, M., El Sanharawi, M., Naud, M.C., van Ijcken, W., Pescini-Gobert, R., Martinet, D., Maass, A., Wijnholds, J., Crisanti, P., Rivolta, C., Behar-Cohen, F., 2015. A new CRB1 rat mutation links Muller glial cells to retinal telangiectasia. The Journal of neuroscience : the official journal of the Society for Neuroscience 35, 6093-6106.

**Table 1.** Primary antibodies used in the present study.

| Target protein | Species | Source* | Cat. No. /clone | Dilution |
|---|---|---|---|---|
| vimentin | mouse | DAKO | V9 | 1:500$^{IF}$ |
| SV40 T-antigen | mouse | Abcam | AB16879 | 1:50$^{IF}$ |
| S100 | rabbit | Sigma-Aldrich | S2644 | 1:50$^{IF}$ |
| GFAP | rabbit | DAKO | Z033429 | 1:100$^{IF}$ |
| GS | mouse | BD Bioscience | 610517 | 1:250$^{WB}$ |
| CRALBP | mouse | Life Technologies | MA1-813 | 1:250$^{WB}$ |
| $\alpha$-tubulin | rat | Novus Biologicals | NB600-506 | 1:2000$^{WB}$ |
| rhodopsin | mouse | Abcam | AB3267 | 1:1000$^{IF}$ |
| blue cone opsin | goat | Santa Cruz | SC-14363 | 1:2000$^{IF}$ |
| tau | rabbit | DAKO | A0024 | 1:5000$^{IF}$ |
| CD11b | mouse | Ab D Serotec | MCA275R | 1:500$^{IF}$ |
| NG2 | rabbit | Merk Millipore | AB5320 | 1:1000$^{IF}$ |
| RPE65 | mouse | Santa Cruz | SC-53489 | 1:1000$^{IF}$ |

*Source location: Abcam, Melbourne, VIC, Australia; Ab D Serotec, Kidlington, UK; BD Bioscience, Franklin Lakes, NJ, USA; DAKO, Sydney, NSW, Australia; Life Technologies Australia, Scoresby, Victoria, Australia; Merk Millipore, North Ryde, NSW, Australia; Novus Biologicals, Littleton, CO, USA; Santa Cruz Biotechnology, Paso Robles, CA, USA; Sigma-Aldrich, Castle Hill, NSW, Australia.
$^{IF}$dilution used for immunofluorescence; $^{WB}$dilution used for western blotting.

**Table 2.** Transfection efficiency of SIRMu-1 and rMC-1 cells.

| Transfection reagent | SIRMu-1* | rMC-1* |
|---|---|---|
| FuGENE HD | 14 ± 7 | 16 ± 1 |
| FuGENE 6 | 7 ± 6 | 6 ± 2 |
| Lipofectamine 2000 | 13 ± 3 | 24 ± 6 |
| PEI† | 12 ± 2 | 15 ± 2 |

* Data are presented as mean ± SD of 3 independent experiments.
† PEI, polyethylenimine.

## Legends

**Figure 1.** Initial characterization of SIRMu and SIRMu-1 cells. Immunocytochemistry was performed on primary (1º) MCs, SIRMu, SIRMu-1 and rMC-1 cells. (**A**) Phase contrast images of cells fixed with 4% paraformaldehyde/PBS. Cells were labelled with primary antibodies targeting (**B**) vimentin and (**C**) SV40 T-antigen. (**D**) Anti-mouse Alexa Fluor 594 secondary (2º) antibody control, in the absence of primary antibody, for B and C. DAPI was used for nuclear staining. Scale bar = 100 µm and applies to all images.

**Figure 2.** Expression of MC markers in SIRMu-1 cells. Immunocytochemistry was performed on primary (1º) MCs, SIRMu-1 and rMC-1 cells, labelled for (**A**) S100 and (**B**) glial fibrillary acidic protein (GFAP). (**C**) Anti-rabbit Alexa Fluor 488 secondary (2º) antibody control, in the absence of primary antibody, for A and B. Scale bar = 100 µm and applies to all images. (**D**) Western blots of 1º MCs, SIRMu-1 and rMC-1 cells, probed for glutamine synthetase (GS) and cellular retinaldehyde-binding protein (CRALBP). Expected band size of each protein is shown in brackets. Arrows indicate target protein bands and asterisks indicate non-specific bands.

**Figure 3.** Immunocytochemical analysis of retinal cell markers on SIRMu-1 cells. Primary (1º) mixed retinal cultures and SIRMu-1 cells were labelled for (**A**) rhodopsin, (**B**) blue cone opsin, (**C**) tau, (**D**) CD11b and (**E**) NG2. (**F**) Anti-mouse Alexa Fluor 594 secondary (2º) antibody control, in the absence of primary antibody, for A and D. (**G**) Anti-goat Alexa Fluor 594 secondary

antibody control for B. (**H**) Anti-rabbit Alexa Fluor 594 secondary antibody control for C and E. (**I**) 1º retinal pigmented epithelial (RPE) cells and SIRMu-1 cells were stained for RPE65. (**J**) Anti-mouse Alexa Fluor 594 secondary antibody control for 1º RPE in I. See F for SIRMu-1 anti-mouse secondary antibody control. DAPI was used for nuclear staining. Scale bar = 100 μm and applies to all images.

**Figure 4.** mRNA sequencing of MCs. (**A**) Multidimensional scaling plot of normalised data for 12 RNA-seq samples. Red circles: primary (1º) MCs (4 biological replicates), Blue squares: rMC-1s (3 replicates), Green diamonds: SIRMu-1s (5 replicates). 2 SIRMu-1 samples grown in the presence of the antibiotic gentamicin and the antifungal amphotericin B are indicated by black dots. (**B**) Bar graph showing numbers of significantly differentially expressed genes which were either upregulated or downregulated at a fold-change of greater than 5 in SIRMu-1 and rMC-1 cells compared to 1º MCs. (**C**) Heatmap showing expression levels of MC marker genes. SIRMu-1 samples grown in the presence of gentamicin and amphotericin B are indicated by asterisks. RPKM, reads per kilobase per million.

**Supplementary materials**

**Supplementary table S1.** Differentially expressed genes (DEGs) by a fold-change of at least 5 relative to primary MCs from RNA-seq data. **(A)** DEGs in both the SIRMu-1 and the rMC-1 cell lines relative to primary MCs. **(B)** DEGs only in the SIRMu-1 cell line relative to primary MCs. **(C)** DEGs only in the rMC-1 cell line relative to primary MCs. Downregulation is indicated by -1, and upregulation by 1.

(Not included in this PDF. This table can be found at https://doi.org/10.1016/j.exer.2019.01.013)

**Supplementary figure S1.** Differentially expressed genes in SIRMu-1 and rMC-1 cells, compared to primary ($1^o$) MCs. **(A)** Venn diagram displaying the number of significantly differentially expressed genes at a fold-change of greater than 5 in each immortalized cell line compared to $1^o$ MCs. **(B)** Gene ontology (GO) analysis of RNA-seq data. Bar graph showing significantly overrepresented (FDR < 0.05) PANTHER GO-Slim Biological Process terms among genes differentially expressed in rMC-1 cells relative to primary MCs, compared to the background *R. norvegicus genome*.

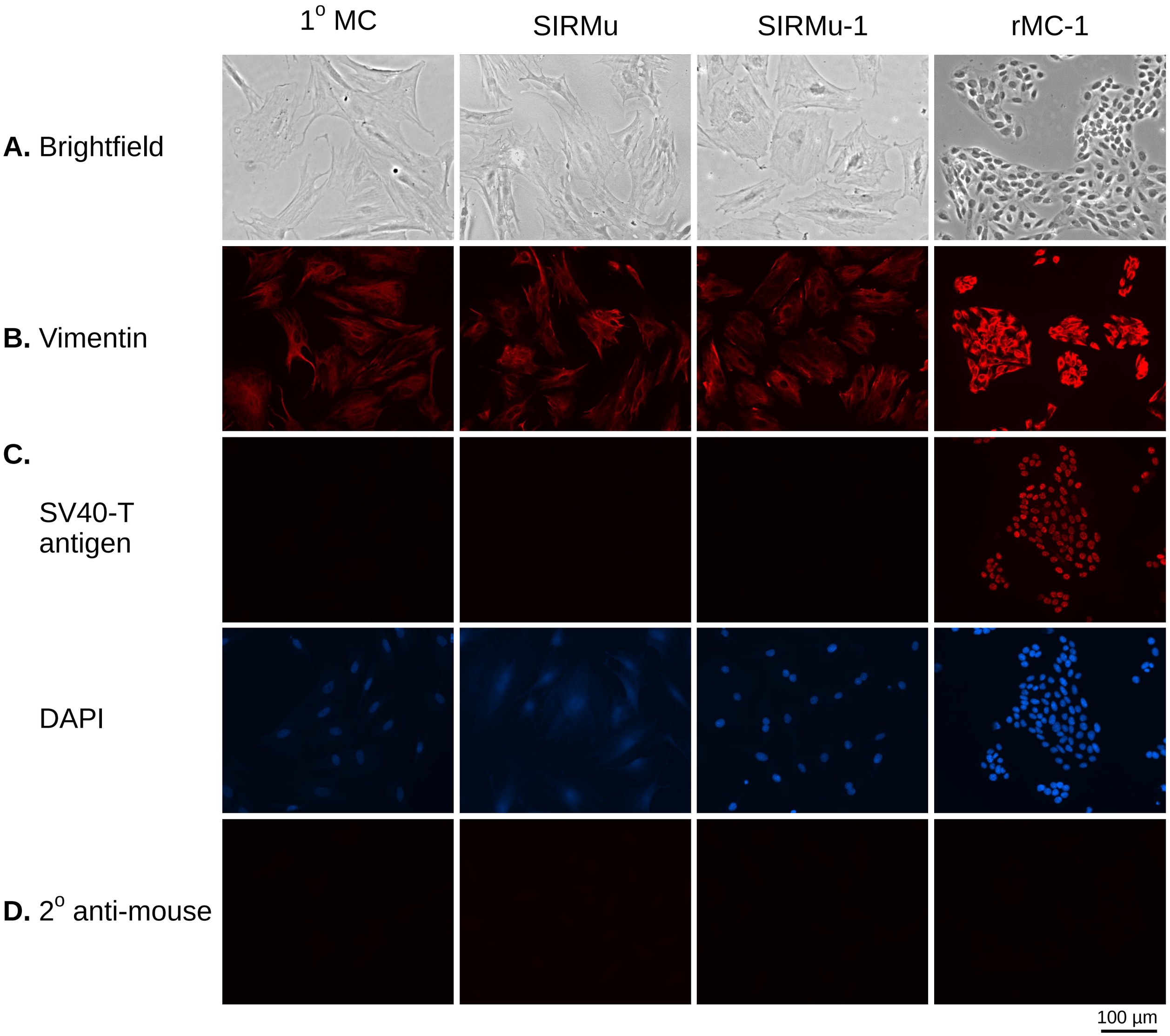
1° MC
SIRMu
SIRMu-1
rMC-1
A. Brightfield
B. Vimentin
C.
SV40-T antigen
DAPI
D. 2° anti-mouse
100 µm

**Figure 1.**

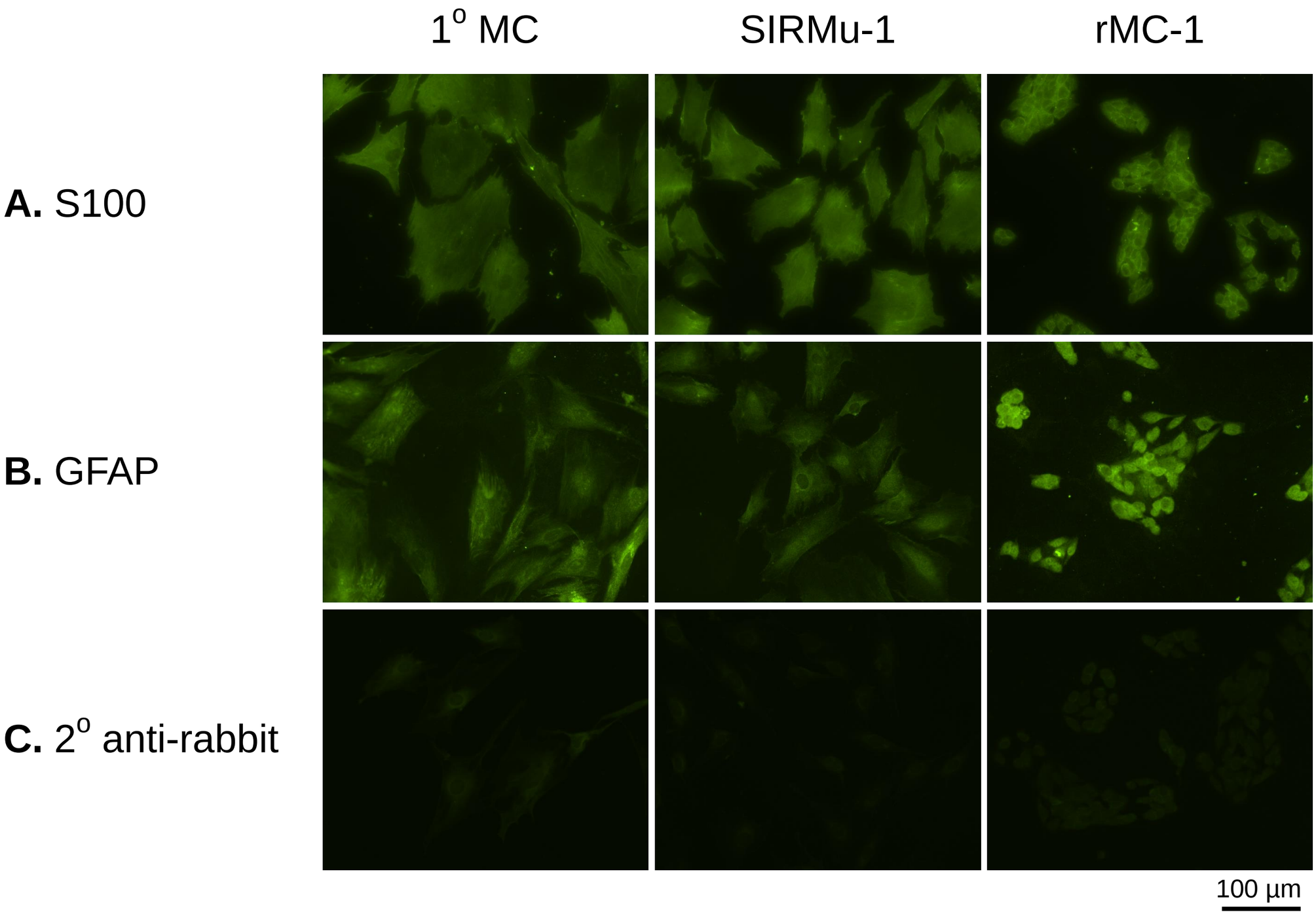
1° MC
SIRMu-1
rMC-1
A. S100
B. GFAP
C. 2° anti-rabbit
100 µm

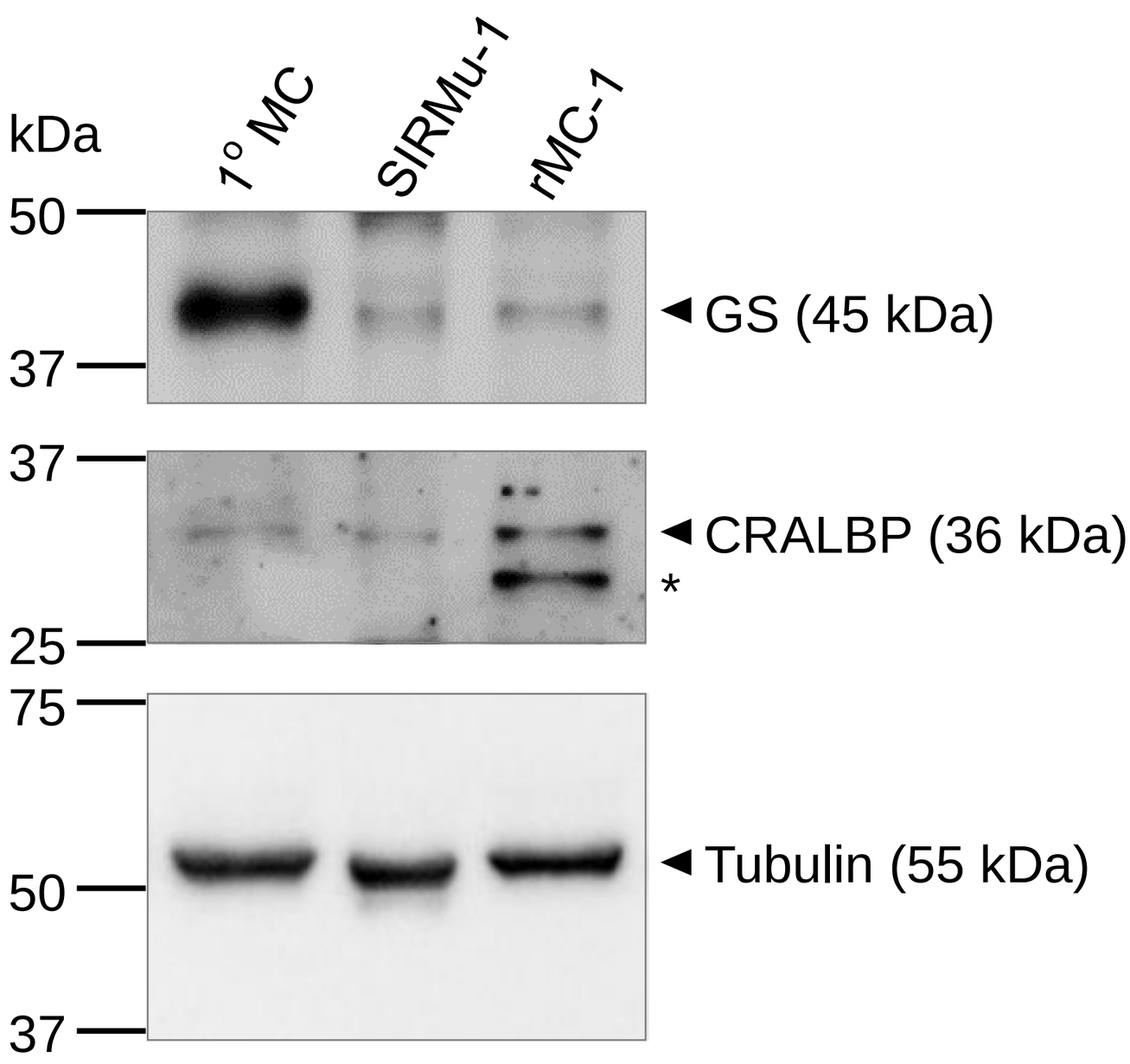
D.
kDa
1° MC
SIRMu-1
rMC-1
50
37
GS (45 kDa)
37
25
CRALBP (36 kDa)
*
75
50
37
Tubulin (55 kDa)

**Figure 2.**

1° mixed retinal SIRMu-1

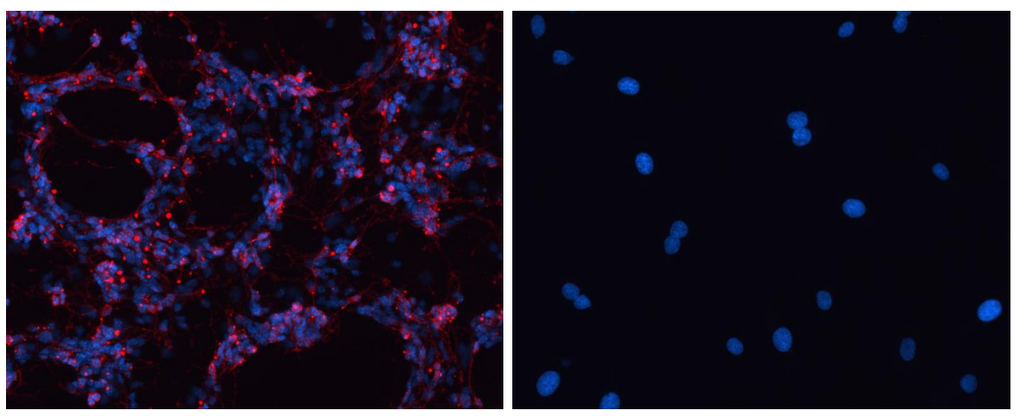

**A.** Rhodopsin

1° mixed retinal SIRMu-1

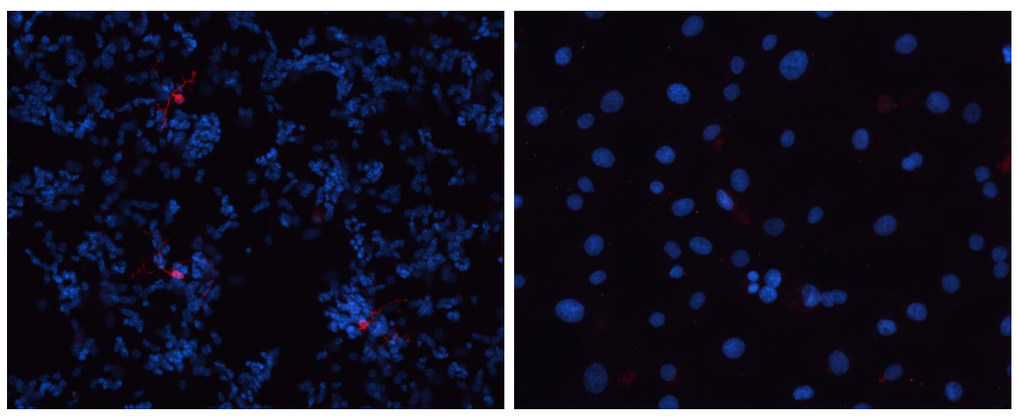

**B.** Blue cone opsin

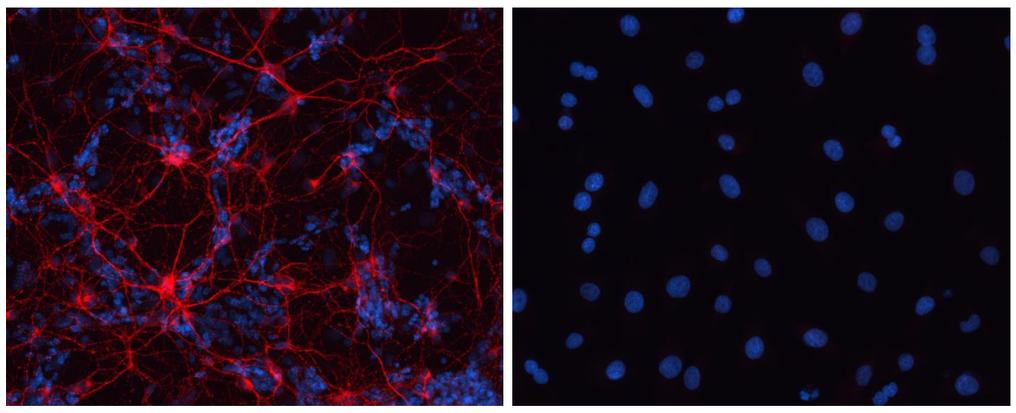

**C.** Tau

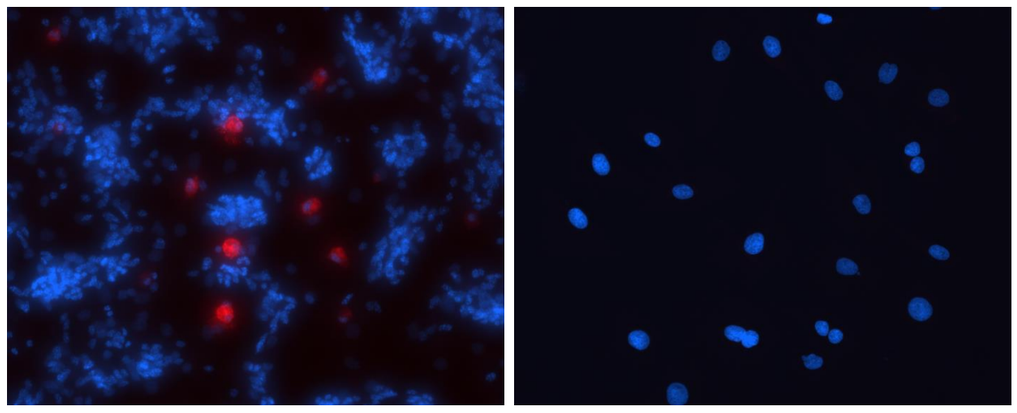

**D.** CD11b

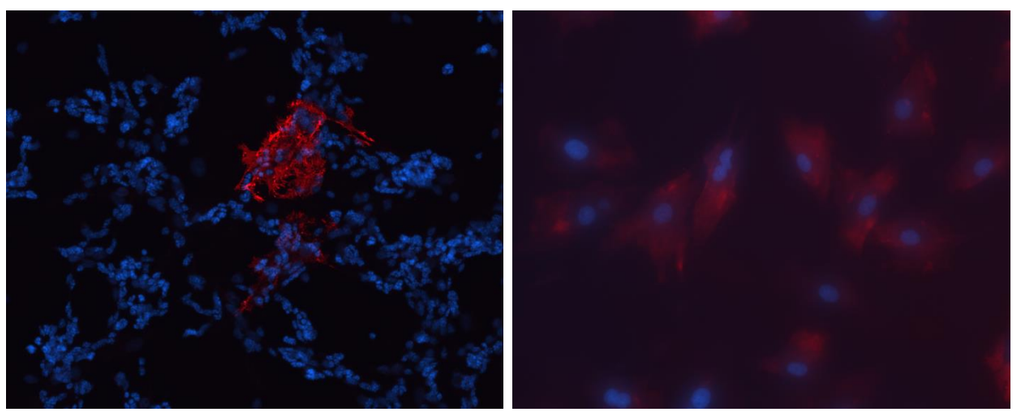

**E.** NG2

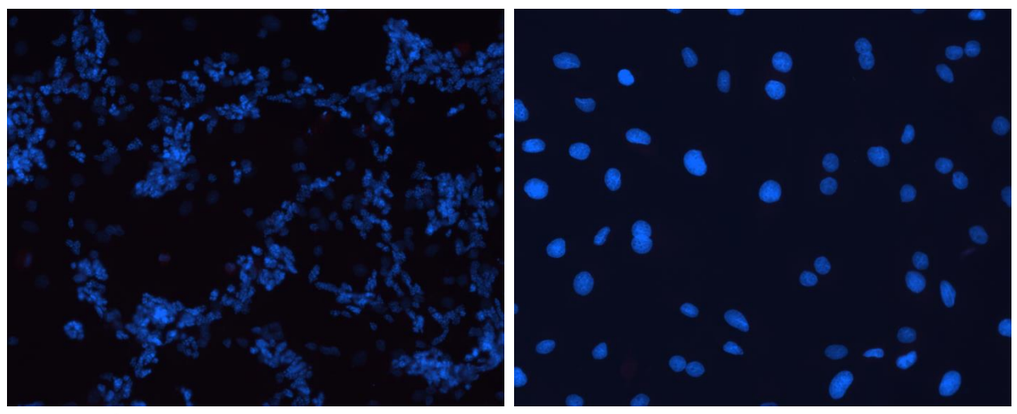

**F.** 2° anti-mouse

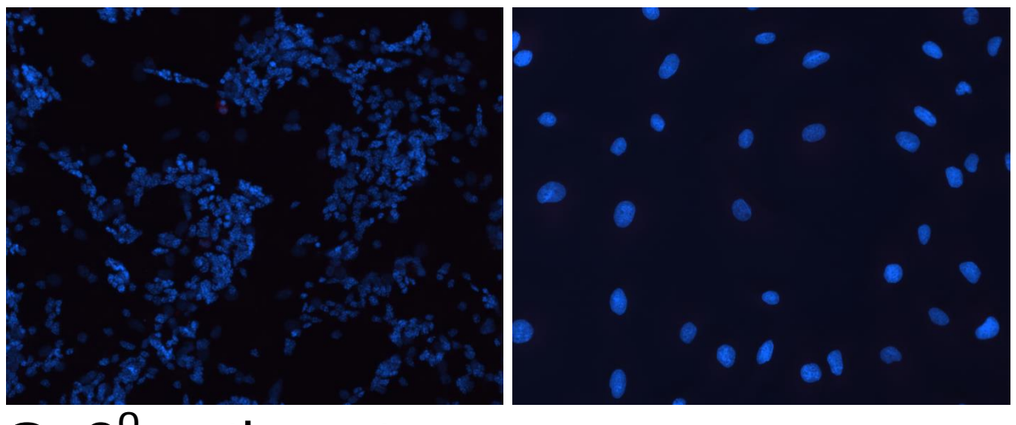

**G.** 2° anti-goat

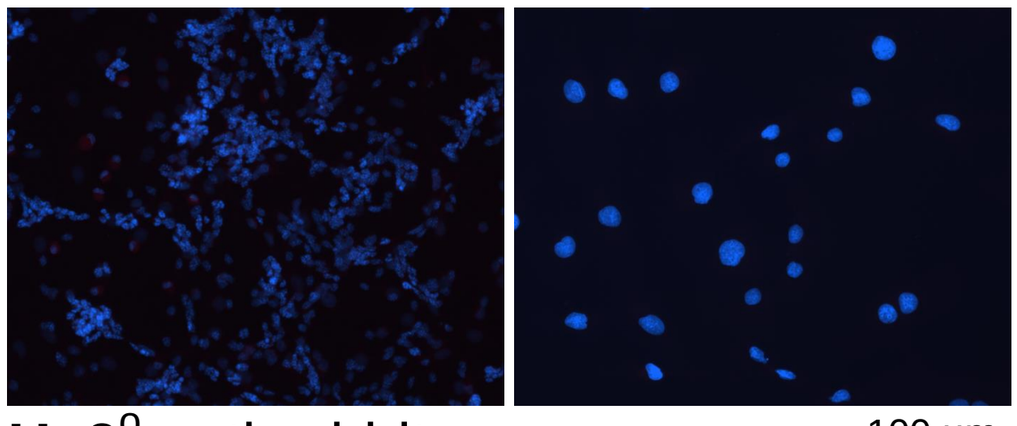

**H.** 2° anti-rabbit

100 µm

1° RPE SIRMu-1

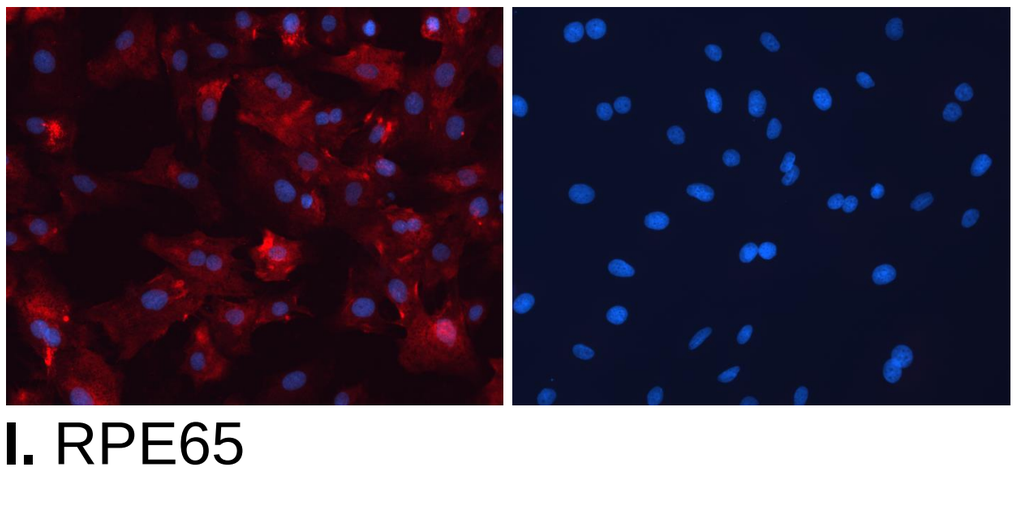

**I.** RPE65

1° RPE

**J.** 2° anti-mouse

**Figure 3.**

**A.**

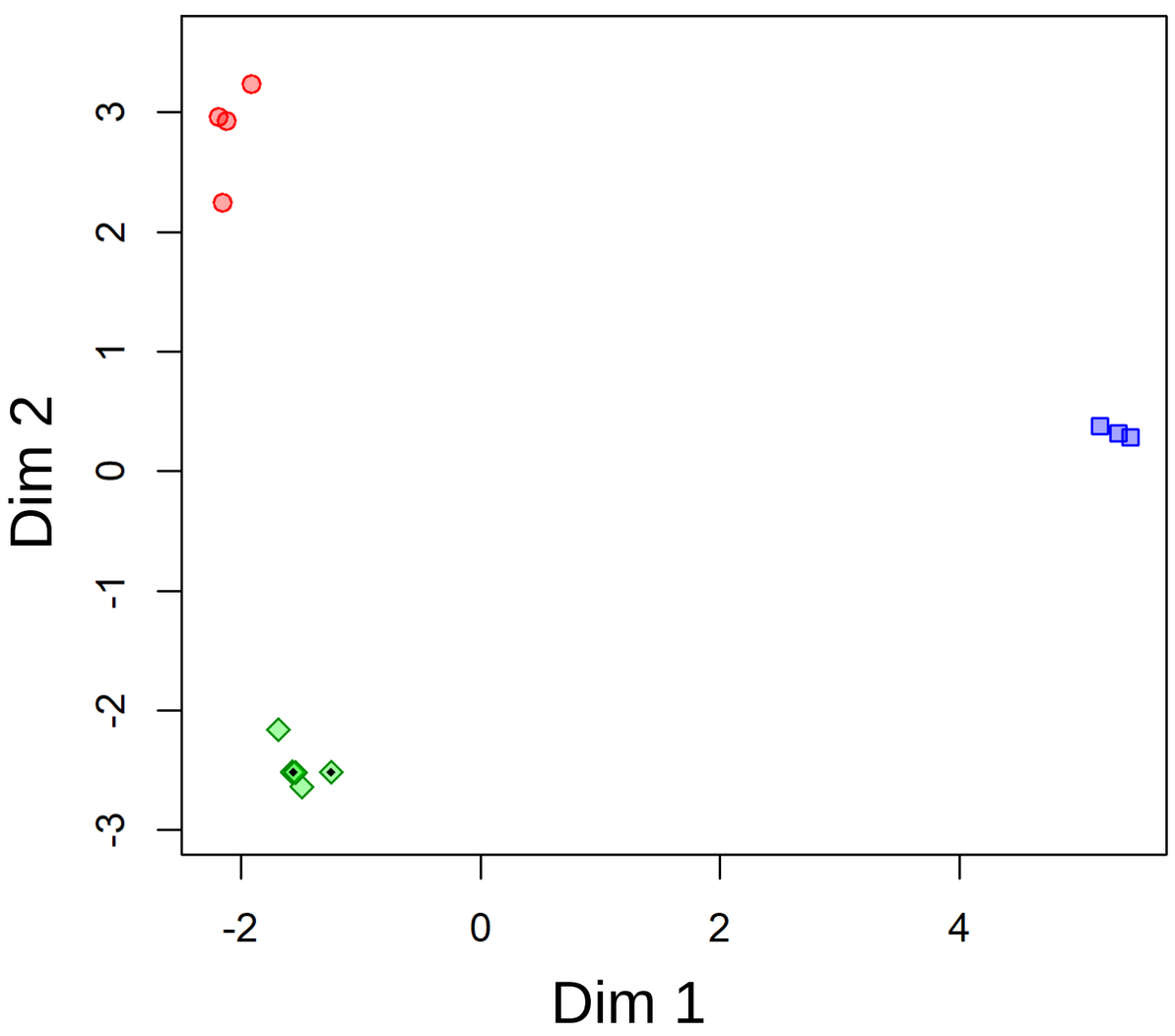
Dim 2
3
2
1
0
-1
-2
-3
-2
0
2
4
Dim 1

**B.**

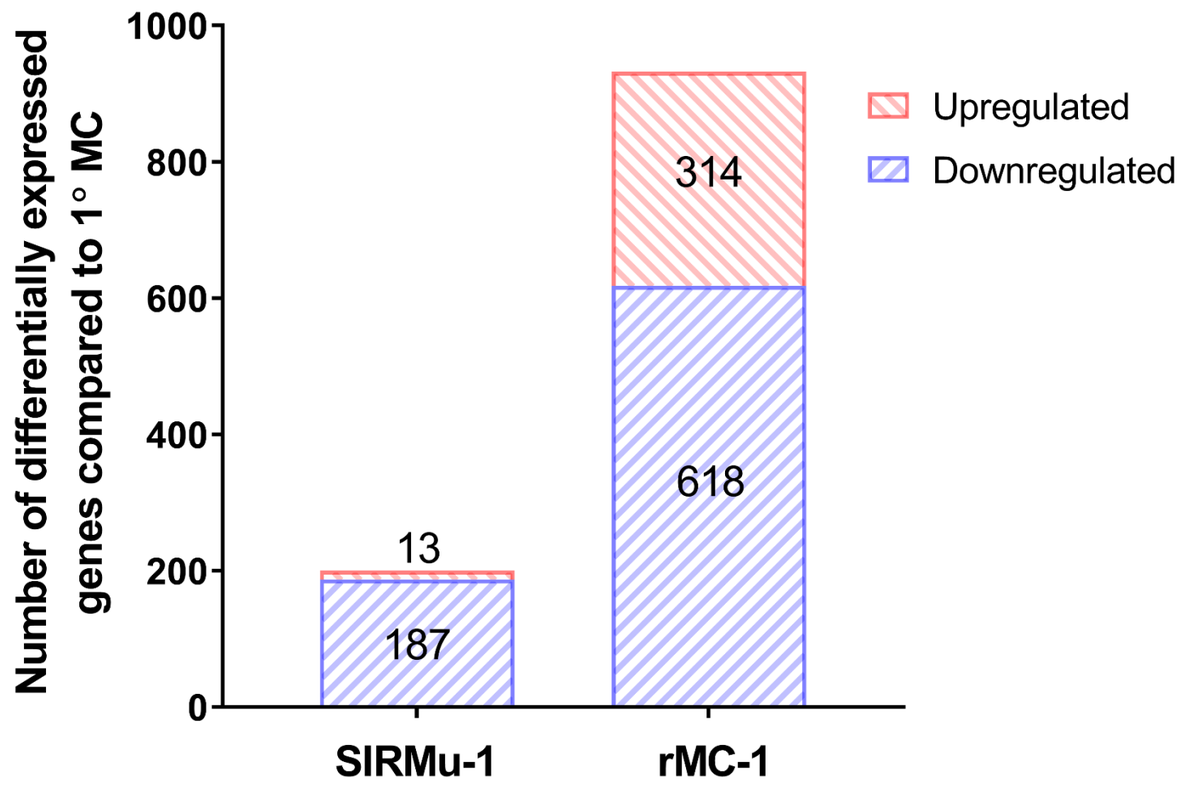
Number of differentially expressed genes compared to 1° MC
1000
800
600
400
200
0
314
618
13
187
Upregulated
Downregulated
SIRMu-1
rMC-1

**C.**

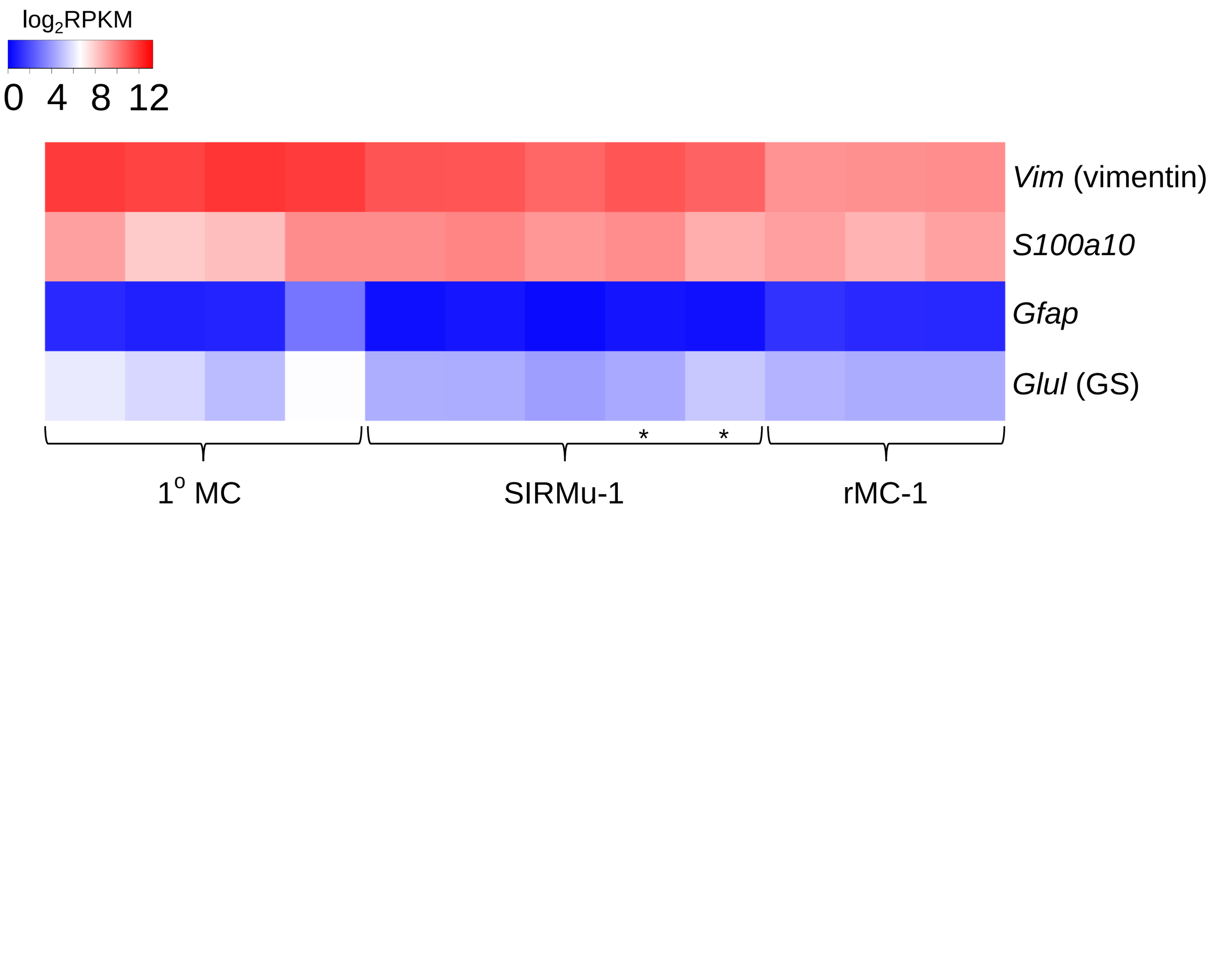
log2RPKM
0 4 8 12
Vim (vimentin)
S100a10
Gfap
Glul (GS)
*
*
1o MC
SIRMu-1
rMC-1

**Figure 4.**

**A.**

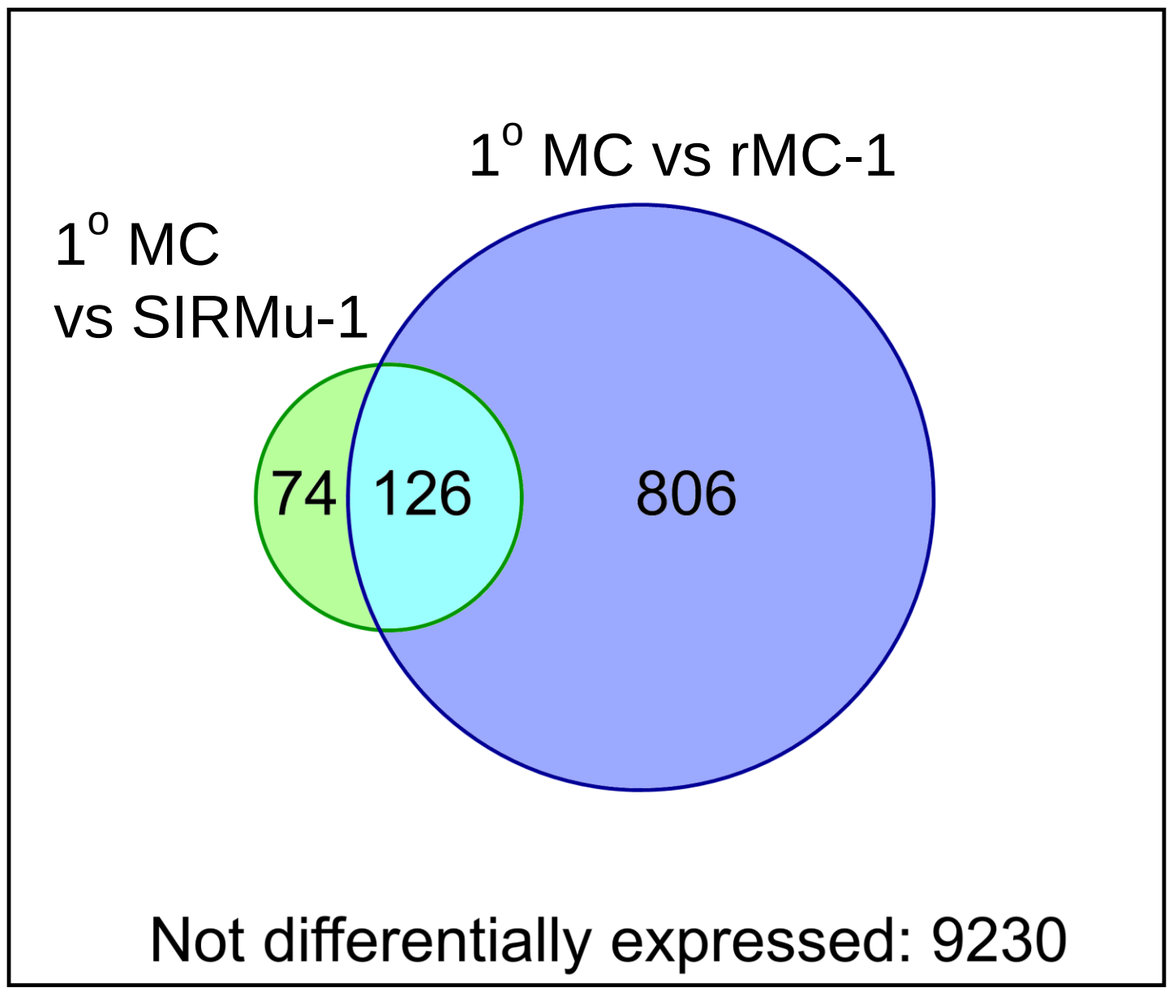


**B.**

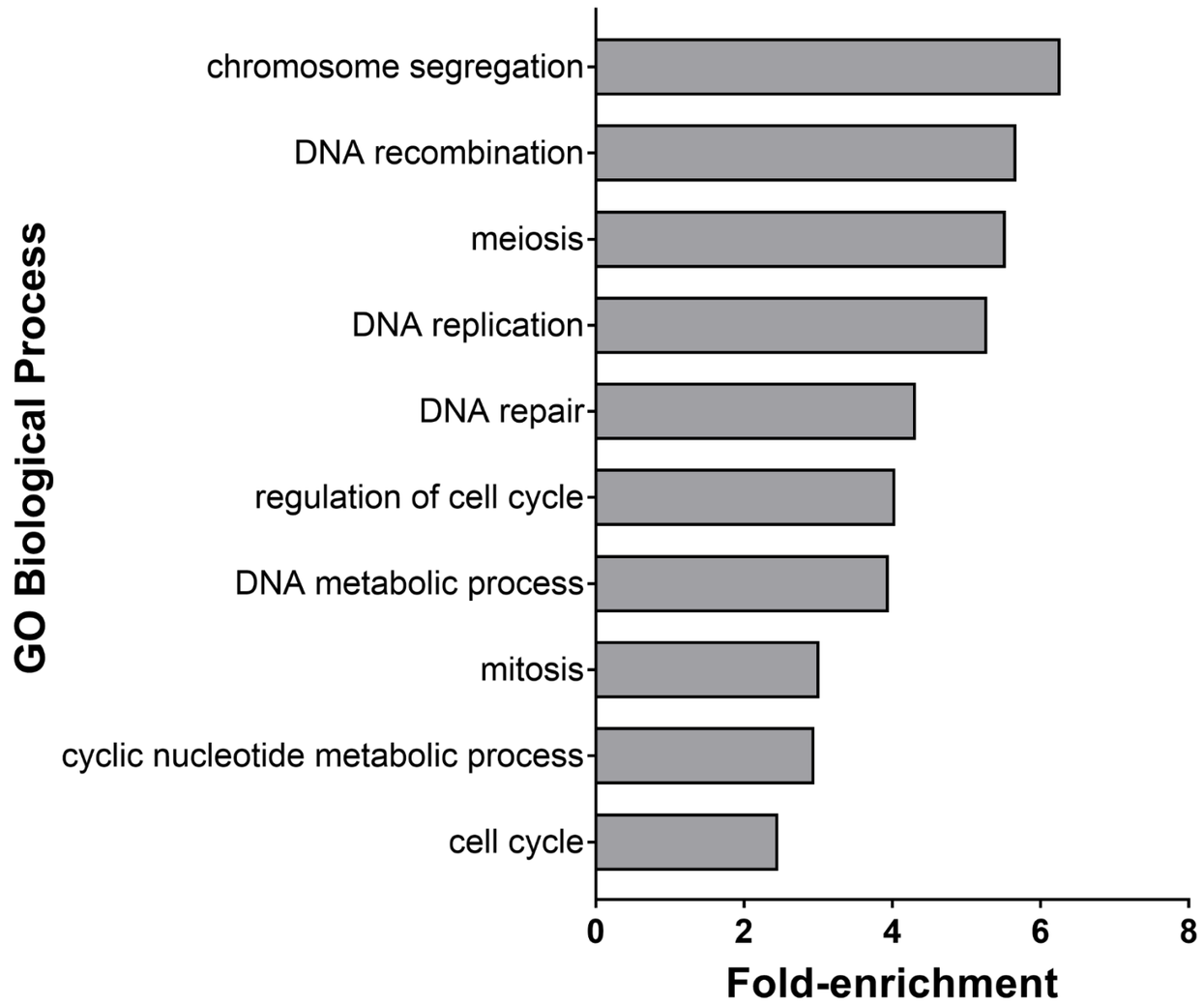


**Supplementary figure S1.**